Local Density Estimation and Dynamic Transmission-Range Assignment in Vehicular *Ad Hoc* Networks

Maen Artimy, *Member, IEEE*

***Abstract*—Vehicular *ad hoc* networks have several characteristics that distinguish them from other *ad hoc* networks. Among those is the rapid change in topology due to traffic jams, which also disturbs the homogeneous distribution of vehicles on the road. For this reason, a dynamic transmission range is more effective in maintaining the connectivity while minimizing the adverse effects of a high transmission power. This paper proposes a scheme that allows vehicles to estimate the local density and distinguish between the free-flow and the congested traffic phases. The density estimate is used to develop a dynamic transmission-range-assignment (DTRA) algorithm that sets a vehicle transmission range dynamically according to the local traffic conditions. Simulations of several road configurations validate the quality of the local density estimation and show that the DTRA algorithm is successful in maintaining the connectivity in highly dynamic networks.**

***Index Terms*—*Ad hoc* networks, connectivity, density estimation, inter-vehicle communications, transmission range, vehicular *ad hoc* networks.**

I. Introduction

NODE DENSITY has a great impact on the performance of vehicular *ad hoc* networks (VANETs) by influencing some factors such as capacity, routing efficiency, delay, and robustness. Waves of traffic jams, whether caused by constraints in the transportation network, traffic controls, or fluctuations in speed, cause the network's density to vary from one location to another, thus disturbing the homogeneous distribution of nodes. Moreover, the abrupt and frequent change in density creates a highly dynamic topology. This topology change would cause severe degradation to the network's performance (increased collisions and interference, excessive broadcasts, too many routing paths, etc.) if the protocols in VANETs were not designed to handle such conditions.

Controlling the communication range by adjusting the transmission power can be used to mitigate the adverse effects of high node density. The choice of the communication range has a direct impact on connectivity, which is a fundamental property of an *ad hoc* network. In a VANET, a static transmission range cannot maintain the network's connectivity due to the nonhomogeneous distribution of vehicles and rapid change of traffic conditions. It is shown in [1] and [2] that a dynamic transmission range is needed to maintain the connectivity in nonhomogeneous networks to take advantage of power savings and increased capacity.

In this paper, we derive a relationship that allows a vehicle to estimate its local traffic density. This relationship is used to develop the dynamic transmission-range-assignment (DTRA) algorithm that adjusts a vehicle's transmission range according to the local traffic conditions. The DTRA algorithm requires no external information (such as vehicle position). Moreover, there is no communication overhead involved since the algorithm uses only the vehicle's internal state to determine the transmission range. The algorithm is transparent to the data communication protocols. Therefore, it can be integrated with the existing systems with little or no change to the latter. The algorithm is highly adaptable to traffic conditions (density and speed) that may change in a very short time due to traffic jams or road constraints.

We used Pipes' car-following model [3], the two-fluid model [4], [5], and the Nagel and Schreckenberg (NaSch) vehicle traffic model [6] as the main analytical tools to derive the relationship for the local density estimate. Simulations of vehicle traffic using RoadSim [7] are employed to validate the quality of the analytical estimates and to measure the performance for the DTRA algorithm in several highway configurations.

The remainder of this paper is organized into the following sections. In Section II, a brief introduction to the relevant topics in traffic theory is provided. Section III describes the NaSch model, the road configurations used in the simulations, and the assumed communications model. Section IV discusses the effect of vehicle density on the minimum transmission range required to maintain connectivity. The density-estimation scheme is provided in Section V. Section VI describes the DTRA algorithm and its performance evaluation. The conclusion is provided in Section VII.

II. Introduction to Traffic-Flow Theory

Traffic-flow theories explore relationships among the main quantities: vehicle density, flow, and speed. The flow q measures the number of vehicles that pass an observer per unit time. The density k represents the number of vehicles per unit distance. The speed u is the distance that a vehicle travels per unit time. The units of these quantities are usually expressed

Manuscript received July 1, 2006; revised November 24, 2006 and February 7, 2007. The Associate Editor for this paper was C. K. Toh.

The author was with Dalhousie University, Halifax, NS B3H 3C3, Canada. He is now with the Internetworking Atlantic Inc., Halifax, NS B3J 1L1, Canada (e-mail: m.artimy@ieee.org).

Digital Object Identifier 10.1109/TITS.2007.895290

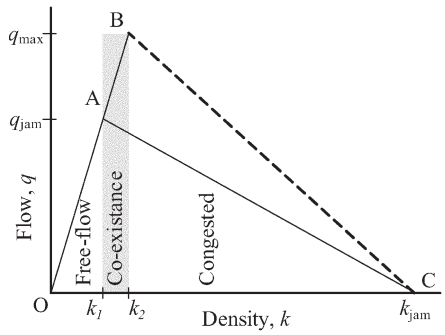

Fig. 1. Fundamental diagram of road traffic (flow–density relationship).

in vehicles per hour per lane (veh/h/lane), vehicles per kilometer per lane (veh/km/lane), and kilometers per hour (km/h), respectively. In general, traffic streams are not uniform, but they vary over both space and time. Therefore, the quantities q, k, and u are meaningful only as averages or as samples of random variables [8]. The three quantities are related by the so-called fundamental relationship [9]

$$q = u \times k. \tag{1}$$

Several theories attempt to define the relationships among each pair of variables in (1), but no single theory provides the complete picture. The following sections provide a brief introduction to the principles that are most relevant to the scope of this paper.

A. Speed–Density Relationship

Car-following models [10] provided an early means to describe the speed–density relationship. These models apply to single lane with dense traffic without overtaking allowed. They also assume that each driver reacts in some specific fashion to a stimulus from the vehicle(s) ahead or behind. The models do not apply in low densities where interactions between the vehicles disappear.

The car-following model proposed by Pipes [3] assumes that drivers maintain constant time headway between vehicles. This model results in the following speed–density relation [9]

$$u = \lambda \left(\frac{1}{k} - \frac{1}{k_{\text{jam}}} \right) \tag{2}$$

where λ measures the sensitivity of the vehicle interaction, and k_{jam} is the maximum vehicle density at traffic jam.

B. Fundamental Diagram of Road Traffic

The fundamental diagram of road traffic describes the flow–density relationship. A typical $q-k$ relationship follows the general shape of Fig. 1. The figure shows that the flow is zero when there are no cars on the road and when there is a complete traffic jam at maximum density k_{jam}. The shape of Fig. 1 suggests that there are two $q-k$ regimes. The left branch O-A of the relationship represents the free-flow traffic at densities below k_1. In the free-flow phase, interactions between the vehicles are rare because of the low density. As a result, vehicles can travel at free-flow speed u_{f}, which is determined by the slope of the left branch $u_{\text{f}} = q/k$.

At densities above k_2, traffic becomes congested and hindered by traffic jams. The $q-k$ relationship of the congested traffic is represented by the right branch A-C. Empirical evidence and traffic simulations suggest that traffic may also be in a coexistence phase. In densities between k_1 and k_2, drivers may accept shorter headway (time gap) between the vehicles, thus achieving the maximum flow q_{m} at the critical density k_2. High fluctuations of speed in this traffic phase may cause a breakdown in the flow and derive the traffic into the congested phase.

At densities higher than k_1, speed can be expressed as a function of density as in (2). By substituting (2) in (1) and accounting for low-density traffic, a piecewise linear $q-k$ relationship can represent the triangle O-A-C of Fig. 1 [9]

$$q = \min \left[u_{\text{f}} k,\ q_{\text{jam}} \left(1 - \frac{k}{k_{\text{jam}}} \right) \right] \tag{3}$$

where $q_{\text{jam}} = q(k_1) \approx \lambda$.

C. Traffic Jams and Phase Transition

Traffic jams are caused by geometric constraints such as an intersection, an accident, or an access ramp. These scenarios can be described by a standard queueing system where the jam at the bottleneck will grow spatially backward if the arrival rate (inflow) is greater than the service rate (outflow) of the bottleneck. The spatial growth can also be described by the theory of kinematic waves [11].

It is also suggested that waves of traffic jams may occur without the presence of obvious constraints but mainly due to fluctuation (noise) in speed. These fluctuations may be caused by bumps, curves, lapses of attention, and different engine capabilities. In moderate traffic flow, a noise of high amplitude may cause the traffic to become unstable, and traffic jams start to appear [12]. This type of traffic jam can be described by the theory of kinematic waves and has been studied extensively using cellular-automata (CA) models [13], [14].

The transition from the free-flow traffic to the congested traffic can be described with the help of the space-time diagram of Fig. 2. A space-time diagram shows the vehicle positions as they would appear in a series of aerial photographs taken at fixed time intervals of a road section and lined-up vertically according to their time index. A vehicle moving at constant speed will appear as a diagonal line in the space-time diagram, while a stationary vehicle will appear as a vertical line.

Fig. 2(a) shows the traffic flow at density lower than k_1 (in Fig. 1), where a vehicle can travel freely without the influence from other vehicles. Fig. 2(b) shows the traffic whose density is in the range $[k_1, k_2]$. At this density, drivers may adapt to the dense traffic by slowing down and maintaining a minimum safety distance. However, high fluctuations in speed by a lead vehicle may break the flow and create traffic jams. A traffic jam appears in Fig. 2(c) as a cluster of vertical lines is moving backward as time progresses. Vehicles that are not caught in

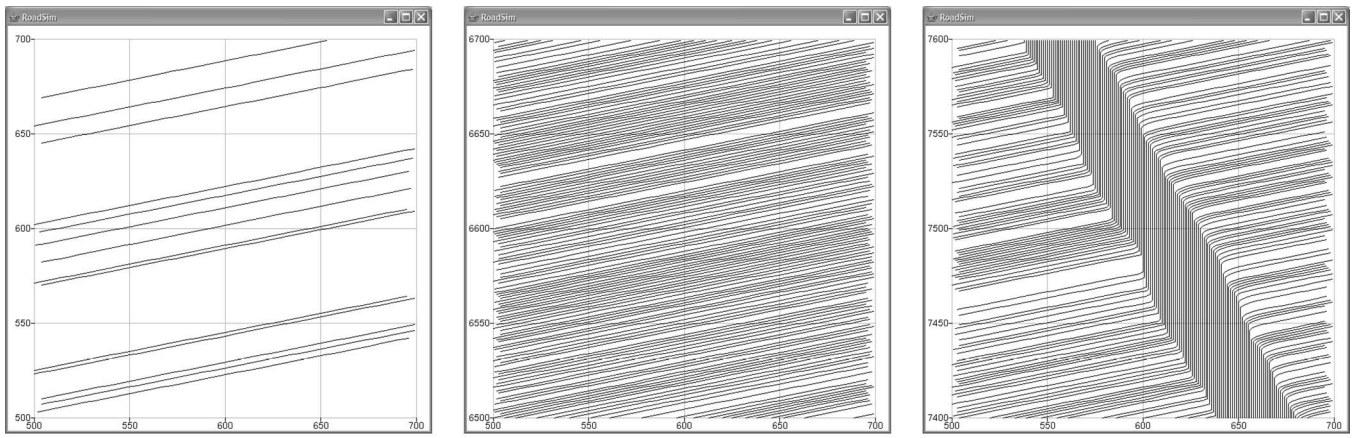

Fig. 2. Space-time diagram illustrating. (a) Free-flow traffic, (b) traffic approaching critical density, and (c) a traffic jam in a 200-m segment (time progresses upward).

jams are traveling in the free-flow traffic. Traffic jams grow as density increases and merge with other traffic jams. Eventually, the entire road section is occupied with one wide traffic jam.

III. Vehicle Network Simulation

The following three sections describe the simulation setup used for this paper.

A. Vehicle-Mobility Model

We used the NaSch vehicle traffic model as the main analytical and simulation tool for this paper. The basic NaSch model [6] consists of a 1-D CA grid of L cells and defines a set of rules for the vehicle's movement through the grid. Each cell represents a small section of the road, which can be either empty or occupied by one vehicle. The vehicle may travel in one direction from one cell to another at the integer speed of $[0, U_{\max}]$, which corresponds to the number of cells that a vehicle can advance in one time step, provided that there are no obstacles ahead. The cell size is chosen to correspond to the reciprocal of maximum vehicle density $k_{\rm jam}$ in traffic jams.

A vehicle's speed is updated in each time step by calculating the gap to the lead vehicle. The gap size determines whether a vehicle can accelerate or slow down. At the end of the step, the vehicle may be moved to another cell according to its new speed. Stochastic behavior is added to the system by slowing down the vehicle randomly. A slightly modified model, which is called the NaSch model with a slow-to-start rule (NaSch-S2S), is known to exhibit phase transition from free flow to traffic jams [13].

We developed a traffic simulator (RoadSim) to generate vehicle-traffic movement based on the NaSch-S2S model [7]. RoadSim adds several extensions to the original model to enable the simulation of multilane traffic and traffic across intersections. RoadSim also generates network graphs, which will be used to determine the minimum transmission-range (MTR) values in the VANET simulations described in Section IV-B.

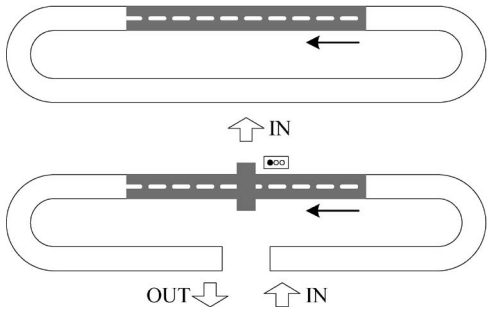

Fig. 3. Highway configurations used to evaluate the local density estimate and DTRA algorithm. (Top) Racetrack configurations (A and B). (Bottom) Intersection configurations (C and D). The data collection is limited to the shaded area.

B. Simulated Highway Configurations

This section describes the four highway configurations that are used in Section V-C to simulate vehicle traffic and evaluate a vehicle's ability to estimate its local density and detect the traffic condition. The same configurations are also used in Section VI-C to evaluate the DTRA algorithm. In all experiments, data are collected from 20 simulation runs.

In two configurations, which are represented by Fig. 3 (top), traffic density is increased gradually in a closed-loop highway so that traffic conditions can change gradually from free-flow to congested traffic. In **Configuration (A)**, vehicles travel in a single-lane highway where overtaking is not allowed. The highway is in the form of a racetrack of 7.5-km length, as shown in Fig. 3 (top). Vehicles enter from a parking facility at a rate (flow) of 60 veh/h and continue to travel around the track indefinitely, which causes the vehicle density to increase until the jam density is reached, and no more vehicles can enter. All vehicles have the same maximum speed of 135 km/h.

The racetrack in **Configuration (B)** allows the vehicles to travel on three lanes and pass each other. Vehicles in this configuration are divided into three classes. Slow vehicles compose 15% of all vehicles, and their maximum speed is set to 81 km/h. Another 15% of vehicles can travel at maximum speed of 135 km/h. The remaining vehicles have a maximum speed of

108 km/h. This distribution reflects the 85th percentile rule that is used as a guide to set the speed limit on highways so that 85% of vehicles will travel below the limit. Note that the maximum speeds are meaningful only in the free-flow traffic. In higher densities, vehicles travel at lower speed, which is unrelated to their maximum speed. The inflow rate of vehicles is set to 300 veh/h. Simulation time for configurations (A) and (B) is 60 000 s.

In the other two configurations, which are represented by Fig. 3 (bottom), the free-flow traffic is interrupted by an intersection, which causes a rapid change in vehicle density across the intersection. **Configuration (C)** consists of a single-lane highway of 7.5 km with a signalized intersection in the middle. Vehicles enter from a parking facility at one end of the highway, at flow of 1800 veh/h, and exit from the other end. The traffic signal has a cycle of 1 min that is divided equally between the red and green phases. In this open-loop highway, a traffic jam occurs upstream from the red light. The choice of the traffic flow and the red time parameters ensures that the traffic jam is created periodically throughout the simulation.

There are two traffic flows in **Configuration (D)**. Nonpriority traffic faces a stop sign at an unsignalized intersection, while the priority traffic can proceed through the intersection uninterrupted. The priority flow is set to $q_{\mathrm{p}} = 900$ veh/h, while the nonpriority flow is set to $q_{\mathrm{n}} = 600$ veh/h. Simulation time for configurations (C) and (D) is 25 000 s.

C. Communications Model

In the discussion of connectivity, the VANET is modeled by a graph. The graph $G = (V, E)$ consists of a set of nodes $V \subset R$ in the Euclidean plane and a set of edges $E \subseteq V^2$. Nodes represent vehicles, whereas edges represent communication links between the vehicles.

It is assumed in this communication model that all vehicles are equipped with wireless transceivers. Vehicles can adjust their transmission power to any value between zero and the maximum power level. The maximum power level is assumed to be equal for all vehicles. An edge (v_i, v_j) may exist if and only if the Euclidean distance between the vehicles v_i and v_j is less than or equal to the shorter transmission range between them, i.e.,

$$E = \left\{(v_i, v_j) \in V^2 |\, |x_i - x_j| \leq \min(r_i, r_j)\right\} \qquad (4)$$

where x_i, r_i are the position and transmission range of the node v_i, respectively. Equation (4) results in an undirected graph. The choice of distance as the primary factor in connectivity is appropriate since the focus of this paper is on the vehicle distribution and density, which both affect the distance among vehicles.

IV. Static Transmission Range

Extensive research is dedicated to determine the MTR required to maintain connectivity in mobile *ad hoc* networks (MANETs). The MTR corresponds to the minimum common value of the nodes' transmitting range that produces a connected communication graph. The motivation behind this research is the difficulty, in many situations, to adjust the nodes' transmitting range dynamically, making the design of a network with a static transmitting range a feasible option.

A. Related Work

VANETs can be modeled as 1-D networks, where nodes (vehicles) are placed along a line. A 1-D network is considered connected if there is no gap wider than the transmission range between any pair of successive nodes. Using this model, Santi and Blough [15] estimate the lower and upper bounds for the transmission range, and Desai and Manjunath [16] provide a probability for gap existence among nodes.

In 1-D networks of infinite size, the transmission range is related to the node density rather than the line's length [17]. Connectivity in infinite networks is limited to short-range communications, and a large-scale *ad hoc* network is not feasible because it is almost surely divided into an infinite number of partitions. The same conclusion also applies to strip networks (networks of infinite length in one dimension and a finite length in the other) [18]. These findings suggest that a VANET should tolerate a certain level of partitioning.

The work presented in [15]–[18] assumes a homogeneous distribution of nodes. It is shown in Sections II and IV-B that this assumption is not always valid in VANETs due to traffic jams and bottlenecks. It is shown in [19] that nonhomogeneous distribution of vehicles results in an increase in the MTR in dense traffic.

In addition to connectivity, the choice of transmission range affects other aspects of VANETs' performance. A longer transmission range may help stabilize the network by increasing the lifetime of communication links, but it has adverse effect on other desirable attributes. Thus, lowering the transmission range to the point where it is just enough to reach an adjacent vehicle reduces the interference range and increases the network throughput linearly [20].

Many studies in VANETs focus on the free-flow traffic in their design and analysis of new protocols (e.g., [21]–[23]). The studies that investigate connectivity either analytically or using simulations also set the traffic conditions to free flow [24], [25]. This choice allows for the greatest flexibility in controlling each of the vehicle traffic parameters (speed, flow, and density) independently. We deal with the entire density range and show that mobility and speed cannot be always considered independent from density.

B. Minimum Transmission Range

In this section, we illustrate the effect of vehicle-traffic characteristics on the MTR when density changes from free flow to a total traffic jam. We should emphasize that increasing the density not only increases the number of vehicles on the road but also creates traffic jams and lowers the average speed of vehicles when the density is higher than some critical density.

In general, the MTR is determined by constructing a minimum spanning tree (MST) among all vehicles in the network. The MTR is the longest edge in the MST [26]. In a single-lane VANET, the MTR is simply the widest gap among vehicles.

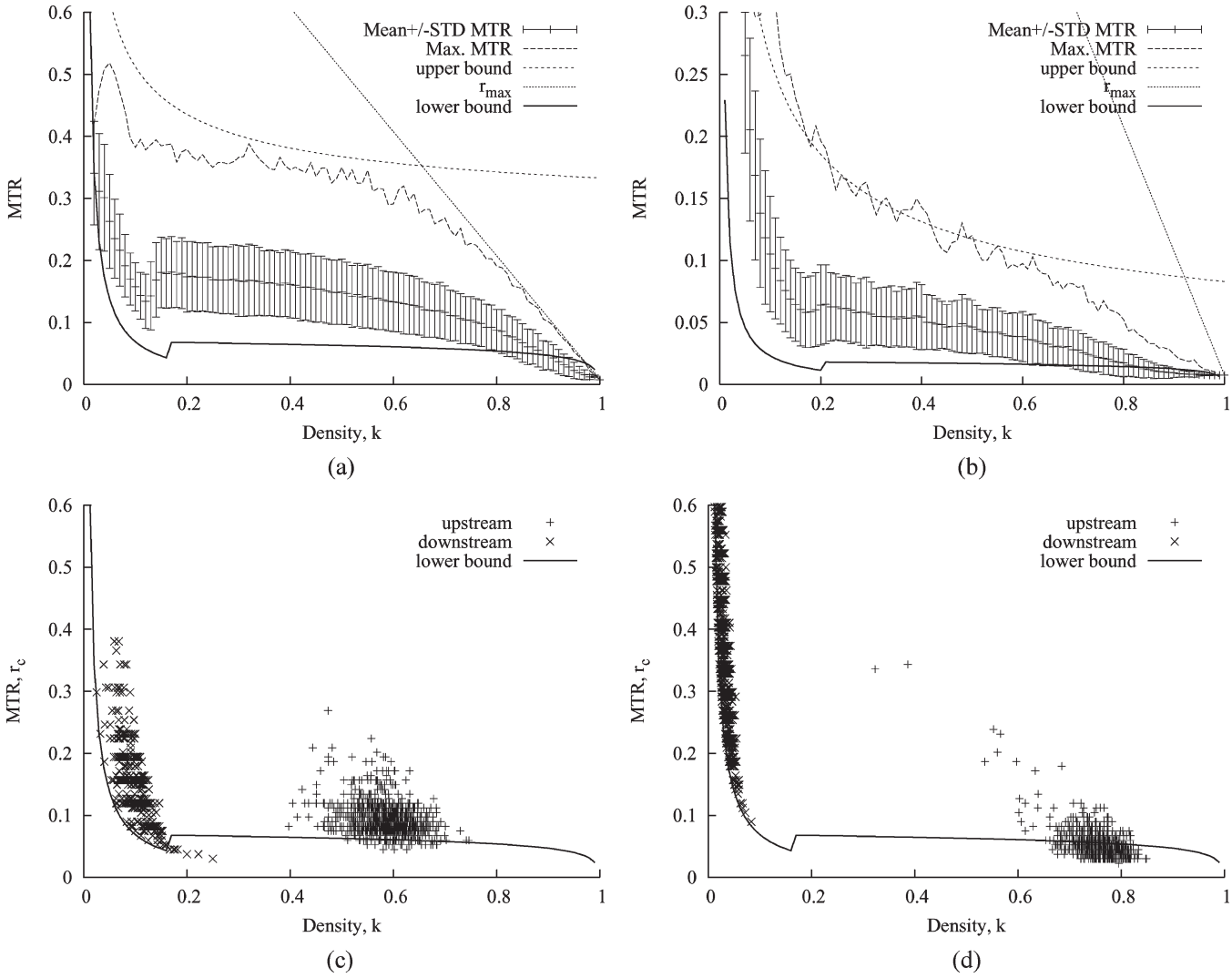

Fig. 4. MTR statistics in (a) one-lane highway segment and (b) three-lane highway segment. MTR values (c) across a traffic light and (d) across a stop sign (only 1% of points are shown to reduce the clutter).

Simulations are used to determine the MTR needed to connect a wireless network among vehicles in the road configurations of Section III-B. The MTR is determined by constructing a spanning tree within the shaded road segments of Fig. 3 in every simulation time step. Then, the MTR value is stored along with the vehicle density within the segment. The data collected from the simulations are classified into 100 density intervals that cover the entire density range. The basic statistics of the MTR are calculated within each energy interval to plot the MTR versus the density values for each scenario.

The solid line in Fig. 4(a) shows the mean value of MTR versus density in the single-lane road configuration. At low densities, the MTR decreases as density increases. At the transition point between the free-flow and the dense traffic, the MTR increases again and then resumes its decline until it reaches its minimum value at a total traffic jam. Fig. 4(a) indicates that despite the higher density, a longer MTR is needed to connect the vehicles beyond the phase transition point of $k_{\mathrm{c}} \approx 1/6$.

The sudden increase in MTR near the point of phase transition is caused by the creation of traffic-jam waves that result in some vehicles being clustered in small areas, while others are spread in less dense traffic, which has the effect of disturbing the homogeneous distribution of vehicles [as shown in Fig. 2(c)]. As density increases, traffic jams increase in size and merge with others until the entire road is occupied by one large traffic jam. Consequently, the MTR decreases until it reaches its minimum value of $1/k_{\mathrm{jam}}$ (the distance between the two vehicles from front bumper to front bumper).

The plot of average MTR and the average maximum MTR are compared with three other relations: The analytical lower bound of MTR in nonhomogeneous traffic is provided by [19]

$$r_{\mathrm{c}}(k) = \begin{cases} \frac{\ln(L)}{k}, & k \le k_{\mathrm{c}} \\ \frac{\ln(L)}{k_{\mathrm{F}}} + \frac{1}{k_{\mathrm{F}}} \ln\left(\frac{k_{\mathrm{jam}}-k}{k_{\mathrm{jam}}-k_{\mathrm{F}}}\right), & k > k_{\mathrm{c}} \end{cases} \tag{5}$$

where k_{F} is the density of the free-flow traffic escaping from a traffic jam and is derived from the maximum speed. The critical density k_{c} separates the free-flow and the congested-traffic modes. Equation (5) was used to emphasize the transition point between the free-flow and the congested traffic phases.

Fig. 4 shows that (5) overestimates the lower bound when the density approaches a wide traffic jam, as explained in [19].

The absolute maximum MTR $r_{\max}$ for a network of finite length L is needed if all but one vehicle is packed at the distance of $1/k_{\text{jam}}$ from each other in one side of the road, while the remaining vehicle is located at the opposite side; therefore

$$r_{\max} = L\left(1 - \frac{k}{k_{\text{jam}}}\right) + \frac{1}{k_{\text{jam}}}. \tag{6}$$

The graph in Fig. 4(a) shows that the average maximum MTR can be approximated by [15]

$$r \leq \sqrt{\frac{L\ln(L)}{k}} + \alpha L. \tag{7}$$

Equation (7) (with $\alpha = 0$) was introduced in [15] as an empirical estimate for the upper-bound MTR in 1-D *ad hoc* network where nodes are assumed to be distributed homogeneously. When applied to the simulation results of the single-lane configuration of Fig. 4, we find that a closer estimate can be obtained by raising the upper bound by a fraction of the road's length $0.25L$. The need for the added term is attributed to the effect of the nonhomogeneous distribution of vehicles.

In the multilane configuration of Fig. 4(b), the critical density is moved higher to $k \approx 1/4$ due to the lower average free-flow speed. The MTR is lower than the single-lane case by a factor of 3 due to the increase in the number of vehicles by the same factor to achieve the same density (per lane). The average maximum MTR can be approximated by (7) with $\alpha \approx 0$.

MTR statistics in the next two configurations are similar to Fig. 4(a). Therefore, instead of showing the statistics, Fig. 4(c) shows a scatter plot of the actual MTR values to emphasize the effect of the abrupt change in traffic conditions from dense traffic behind a red light to free flow a few seconds after the light turns green. This situation is shown in the figure by the presence of two clusters of MTR values. The clusters at high and low densities correspond to the highway segments upstream and downstream from the intersection, respectively. The gap between the clusters indicates that the transition between the two densities is abrupt and takes the form of a shock wave [11]. Fig. 4(d) shows similar results, although the delay encountered by the vehicles upstream of the intersection is random and caused by the wait for priority traffic to clear. The last two configurations emphasize the rapid change of topology in VANETs and the importance of detecting the local traffic conditions in order to adapt the operation of the communication network accordingly.

V. Detection of Local Traffic Conditions

In this section, we derive a relationship for local density estimate based on the car-following model (Section II-A), the NaSch-S2S model (Section III-A), and the two-fluid model (discussed later). This paper represents a novel approach to density estimation that depends only on the vehicles' mobility pattern. Compared to elaborate systems such as [27], the density estimate derived here does not require any exchange of information among vehicles or with a central infrastructure.

Moreover, this section shows that a vehicle can distinguish between the free-flow and the congested traffic conditions by monitoring its own fraction of stopped time. This value serves as an order parameter to detect the local traffic condition. This can be significant in identifying the density region where the local density estimate is valid.

A. Estimation of Local Density

Car-following models suggest a number of relationships between the average speed and density of vehicles such as the Pipes' equation (2). From such relationships, the average vehicle speed can be expressed as a function of density

$$u = u(k). \tag{8}$$

In addition, the two-fluid theory relates the fraction of vehicles that are stopped in traffic f_s to the average speed of all vehicles (including vehicles that are stopped due to traffic conditions but not parked vehicles) [4], [5]

$$u = u_{\max}(1 - f_s)^{\eta+1} \tag{9}$$

where η is a parameter that indicates the quality of service in the transportation network. The value of f_s can be measured by an external observer counting the number of vehicles in the traffic. Note that intentionally parked vehicles are not considered part of the traffic. Instead, they form a part of the street configuration [4].

Moreover, the two-fluid theory relates the stopping time T_s of a test vehicle circulating in a network during a trip of time T_t to the average fraction of stopped vehicles by [4], [5]

$$f_s = \frac{T_s}{T_t}. \tag{10}$$

Equation (10) represents an ergodic principle embedded in the model, i.e., the network conditions can be represented by a single vehicle appropriately sampling the network. Because of this property, a vehicle is able to estimate the density of the surrounding traffic.

To proceed with the derivation of the density estimate, assume that the speed–density relationship is given by (2). This is a reasonable assumption given that the equation is derived from a constant headway car-following model (in which drivers try to maintain a minimum safety headway), and it closely matches the speed–density relationship of the NaSch-S2S model.

From (2), the normalized vehicle density k' is given by

$$k' = \left(\frac{u'}{\lambda'} + 1\right)^{-1} \tag{11}$$

where $k' = k/k_{\text{jam}}$, $u' = u/u_{\max}$, and $\lambda' = \lambda/(u_{\max}k_{\text{jam}})$, respectively.

From (9) and (10), the normalized average vehicles' speed is

$$u' = \left(1 - \frac{T_s}{T_t}\right)^{\eta+1}. \tag{12}$$

TABLE I
CALCULATED VALUES OF λ, k_1, AND k_c

Road configurations	$U_{\max} = 135km/hr$	$U_{\max} = 81km/hr$
λ	0.5557	0.6004
k_1	0.0911	0.1433
k_c	0.1667	0.2500

Equation (12) can be substituted in (11) to provide the means for a vehicle to estimate the density of the surrounding traffic by monitoring its own stopping time. The resultant local density estimate is denoted K. Therefore

$$K = \left[\frac{(1 - T_s/T_t)^{\eta+1}}{\lambda'} + 1\right]^{-1}. \tag{13}$$

The difference between the density obtained from (13) and the one obtained directly from (11) is that the latter provides the global traffic density in a highway segment. Measuring this density requires information about the average speed of vehicles located within the segment, which cannot be obtained without the assistance of an external observer or an elaborate information exchange among the vehicles, such as in [27]. The local density estimate K, on the other hand, depends only on the traffic pattern of the vehicle performing the estimation, given by T_s/T_t, and reflects the local traffic conditions surrounding the vehicle.

Before estimating vehicle density using (13), the values of η, λ, and T_t must be determined. Both η and λ reflect the traffic service level of the road and can be determined statistically or by simulations. Our simulations (not reported here) show that in highway scenarios, $\eta \approx 0$ and $1/\lambda \approx 1.8s$, which is linked to the safety time headway between vehicles that results in a flow of just above 2000 veh/h/lane (q_{jam} in Fig. 1). Both values were also determined analytically for the NaSch-S2S model in [28], as shown in Table I. Reference [4] uses time-lapse aerial photography to determine several traffic parameters, including η, in an urban environment. The choice of the trip time T_t is discussed further in Section V-B.

Equation (13) inherits the limitations of the car-following model, which means that it cannot provide an estimate of density in free-flow traffic where there are no interactions between vehicles. Therefore, a vehicle should be able to identify when the estimate is valid.

B. Fraction of Stopped Vehicles as an Order Parameter

The state of vehicle traffic can be detected using the fraction of stopped vehicles (10) as an order parameter since it exhibits similar characteristics [12]. In free-flow traffic, all vehicles are moving ($f_s = 0$). Once a traffic jam is created, vehicles stop when they join the traffic jam at its end, while other vehicles at the front accelerate away from the traffic jam. From an external observer's perspective, there is always a fraction of vehicles that are stopped completely ($f_s > 0$).

From a single vehicle perspective, only the presence of a local order (a local traffic jam) is detectable if T_s/T_t is used. This provides useful information since a vehicle in a VANET is most affected by its local conditions (e.g., contention during access to a shared communication channel). Therefore, a vehicle may use the value of T_s/T_t directly to detect whether it is traveling in free-flow or congested traffic.

Note that the use of the ratio T_s/T_t to estimate density offers a couple of practical advantages over the use of the vehicle's speed directly in (11) (assuming that speed is ergodic): 1) The stopped time is easily measured, and it is independent of the vehicle's speed; and 2) the speed capabilities are different among vehicles, which results in different density estimates within the same traffic condition.

Equation (10) is implemented as a moving average filter of the speed samples u_τ obtained from the speed sensor of a vehicle at regular time intervals. The order parameter is given by

$$f_{s,\tau} = \frac{1}{T_t} \sum_{i=0}^{T_t - 1} \delta(u_{\tau - i}) \tag{14}$$

where $f_{s,\tau}$ is the fraction of stopped vehicles at time τ, and $\delta(\cdot)$ is the unit impulse function ($\delta(0) = 1$).

Given the interpretation of f_s as the moving average filter of the vehicle status (stopped versus moving), the choice of window size T_t affects two filter properties: the reduction of noise and the step response. To ensure that a vehicle is able to detect and react quickly to the change in traffic conditions, the value of T_t should be on the order of a few seconds. However, a small value of T_t results in a noisy estimate of the order parameter. Considering that vehicles in highway traffic are expected to be constantly moving, any brief stops should indicate traffic congestion. Trial simulations show that a choice of $T_t = 10$ s results in a high correlation between the actual density and its estimated value by vehicles in the highway configurations described in this paper.

C. Evaluation of Density Estimation

Simulation of highway segments are used to determine whether (10) and (13) can provide a reasonable indication of change in traffic conditions and estimate the density. In the simulations, vehicles calculate the ratio T_s/T_t and K in every simulated time step. This information is later compared with the actual density from an observer's perspective. Since vehicle density changes over space and time, the measure of the density over the entire road segment does not reflect the local traffic conditions experienced by vehicles. Therefore, local densities are measured over short road segments.

To verify the validity of (10) as an order parameter, the number of vehicles N and the number of stopped vehicles N_s are counted in a small section of length 37.5 m every simulation time step. Then, block measurements of 120 time steps are used to obtain a single value of the fraction $f_s = N_s/N$. The values of f_s, are plotted versus the density value k, which is obtained in the same road section. Fig. 5 summarizes the results for three road scenarios similar to configurations (A) and (B) in Section III-B: a one-lane road where vehicles have a maximum speed of $U_{\max} = 135$ km/h or $U_{\max} = 81$ km/h and a three-lane road where vehicles have a maximum speed of $U_{\max} = 135$ km/h.

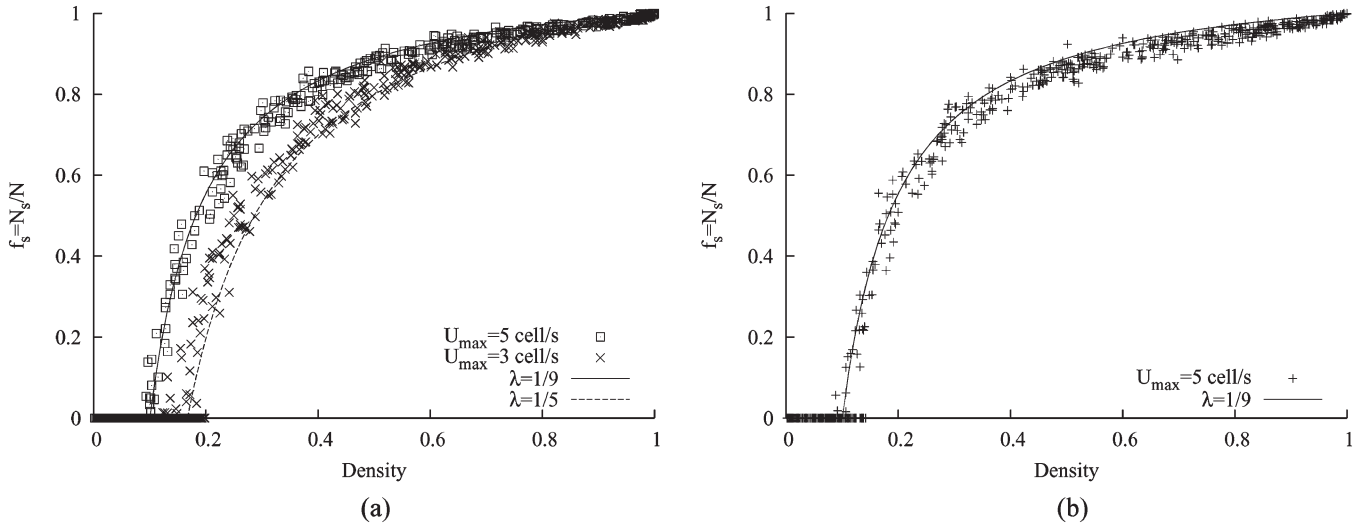

Fig. 5. Order parameter ($f_s = N_s/N$) in (a) one-lane road and (b) three-lane road.

Data points in all cases are compared with the function

$$f_s = 1 - \lambda\left(\frac{1}{k} - \frac{1}{k_{\text{jam}}}\right) \tag{15}$$

which is obtained from the speed–density relationship (2) by replacing u with $1 - f_s$. Table I lists the values of λ used in each scenario. Note that the value of $1/\lambda$ is linked to the safety time headway between vehicles that results in a flow of $q(k_1)$ 2000 veh/h/lane.

The data points in Fig. 5 are shown without averaging to illustrate the presence of the coexistence traffic state. In this figure, the value of f_s rises above zero starting from density k_1 (see Section II); however, in some instances, the free-flow traffic ($f_s = 0$) may exist in densities up to $k_c > k_1$, beyond which, the high density does not allow free-flow traffic.

The observations in Fig. 5 and Table I support the discussion of Section V-A. The value of $f_s = N_s/N = T_s/T_t$ can be used to distinguish between the free-flow and congested traffic conditions.

To determine whether (13) can provide an accurate estimate of the local density, vehicles calculate K in every simulation time step. This information is compared with the actual local density from an observer's perspective. Since vehicle density changes over space and time, the measure of the density over the entire highway segment does not necessarily reflect the local traffic conditions experienced by vehicles at a given location. Therefore, to provide accurate measurement of local densities, a highway segment of 134 cells (1005 m) [the shaded area in Fig. 3 (top)] is divided into short sections of 20 cells (150 m) each. The density in each of these segments is determined independently in every time step.

Fig. 6 shows that the $K - k$ relation deviates from a straight line at densities within the free-flow range ($k < 1/6$ for one-lane configuration and $k < 1/4$ for three-lane configuration). Within this range, (13) has a constant value of ≈ 0.1 when $T_s = 0$ (the vehicle is in constant motion). At higher densities, the estimate K approaches the $K = k$ line in both road configurations.

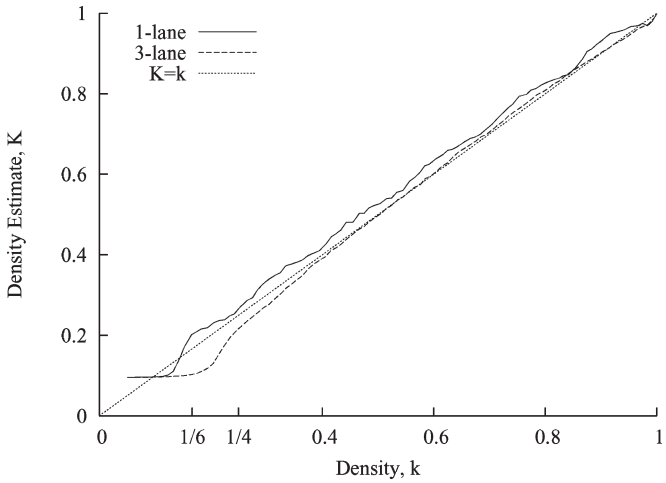

Fig. 6. Density estimate K versus actual density k in one- and three-lane roads.

VI. Nonhomogeneous Transmission-Range Assignment

The topology of an *ad hoc* wireless network is the set of communication links between node pairs used to exchange information packets. Unlike wired networks, the topology of a wireless network may change form due to some uncontrollable factors such as node mobility, weather, interference, or noise. The topology can also be shaped by controlling some parameters such as transmission power and antenna direction [2].

A. Related Work

Power control techniques are considered in the literature for throughput enhancement, link quality protection, Topology Control (TC), power conservation and/or a combination of them. The power control at the Medium Access Control

(MAC) layer can effectively increase the throughput by allowing more concurrent transmissions in the network if the designed protocol carefully maintains connectivity. Since the transmission power controls the bit error rate at the receiver, it helps to maintain the quality and reliability of the wireless link. Moreover, power control can also be employed as a power saving mechanism in order to extend the lifetime of the power-limited nodes.

An ideal power control protocol should be fully distributed, asynchronous, and use local information. In general, there is a tradeoff between the quality of information used by the protocol (such as timely and accurate node positions) and the cost (additional hardware) or overhead (exchange of messages) required [29].

There are several approaches to distributed TC that result in nonhomogeneous transmission-range assignments. In the location-based approaches [2], [30], the nodes are assumed to be able to obtain exact node locations. This information can be exchanged between nodes and used to build an optimum topology in a fully distributed manner. The drawback to this approach is that it requires location information that can be provided only by an additional hardware (e.g., GPS) and/or message overhead.

In the direction-based approaches, a receiver is assumed to be able to determine the direction of the sender when receiving a message. In [31] and [32], it is shown that the network connectivity can be guaranteed if there exist at least one neighbor in each cone of a certain angle centerd at the node. The neighbor-based approach is based on maintaining the number of neighbors reached by a node within certain thresholds by adjusting the transmission power [33]. This approach is simple but does not guarantee connectivity.

The effect of mobility on these schemes is the message overhead generated to update the nodes' transmitting range in response to the change of topology. The amount of this overhead depends on the frequency of topology change. Therefore, it is intuitive that a mobility-resilient topology control protocol should be based on a topology that can be computed locally and requires little maintenance in the presence of mobility. Many of the topology control protocols presented in the literature meet this requirement. However, only some of them have been defined to explicitly deal with node mobility [29]. The protocols [2], [33] are explicitly designed to deal with node mobility. They are zero-overhead protocols since the estimation of the number of neighbors is based on the overhearing of data and control traffic.

Our approach to dynamic range assignment is closely related to a class of topology control algorithms that control a node's degree (number of neighbors) by adjusting the transmission power [34]. These protocols depend on an exchange of information such as in [30] or on some protocol feature as in [35]. Our algorithm, on the other hand, depends only on a vehicle's mobility and does not require any exchange of messages.

B. Dynamic Transmission Range Algorithm

The DTRA algorithm is a Transmission Power Control (TPC) mechanism that employs information about the local vehicle density estimate and the local traffic condition (free-flow versus congested traffic) to set a vehicle's transmission range dynamically. In the DTRA algorithm, no information about neighboring nodes is collected, and no central authority is required. A vehicle can determine its transmission range based on its own mobility pattern, which provides hints about the local traffic density. In this regard, the algorithm is related to a class of algorithms that require no message exchange for their operation. However, unlike these protocols that depend on overhearing of data and control traffic to determine the transmitting power level [2], [33], [35], the DTRA algorithm depends on estimation of vehicle density. As a result, the protocol is transparent to data communication protocols and can be used in conjunction with existing protocols.

It can be concluded from the results of Section IV-B that if all vehicles had to use a homogeneous transmission range for communication, the range should keep the vehicular network connected in all traffic conditions. This can be achieved only if the transmission range is wide enough to accommodate conditions such as free-flow traffic and traffic across intersections.

Alternatively, estimation of traffic density provides the necessary means to develop a TPC algorithm to set a vehicle's transmission range dynamically as traffic conditions change. In its basic form, the algorithm maps the time-varying values of T_s/T_t into a transmission range r at regular time intervals

$$r = D(T_s/T_t). \tag{16}$$

Algorithm 1 Dynamic Transmission-Range Algorithm.

Input α, λ' ▷ constants
Input MR ▷ maximum transmission range
1: **function** $\mathrm{D}(T_s/T_t)$
2: $f_s \leftarrow T_s/T_t$
3: **if** $f_s = 0$ **then** ▷ free-flow traffic
4: TR $\leftarrow$ MR
5: **else** ▷ congested traffic
6: $K \leftarrow [(1 - f_s)/\lambda' + 1]^{-1}$
7: $t_1 \leftarrow \mathrm{MR} \times (1 - K)$
8: $t_2 \leftarrow \sqrt{\mathrm{MR} \times \log(\mathrm{MR})/K} + \alpha \times \mathrm{MR}$
9: TR $\leftarrow \min(t_1, t_2)$
10: **end if**
11: **return** TR ▷ dynamic transmission range
12: **end function**

Algorithm 1 provides one implementation of the mapping function (16). The transmission range is set to its maximum level in free-flow traffic. In congested traffic, r is determined by (6) and (7). Fig. 7 shows that the minimum of the values returned by these two equations represents the transmission range needed in congested traffic. In general, $D(\cdot)$ may depend on other factors such as the desired level of path redundancy or the percentage of equipped vehicles.

Algorithm 1 requires three constants, which are considered design parameters. The value of αL [from (7)] is used to fine-tune the value of transmission range returned in congested traffic. The effect of this parameter is discussed in Section VI-C.

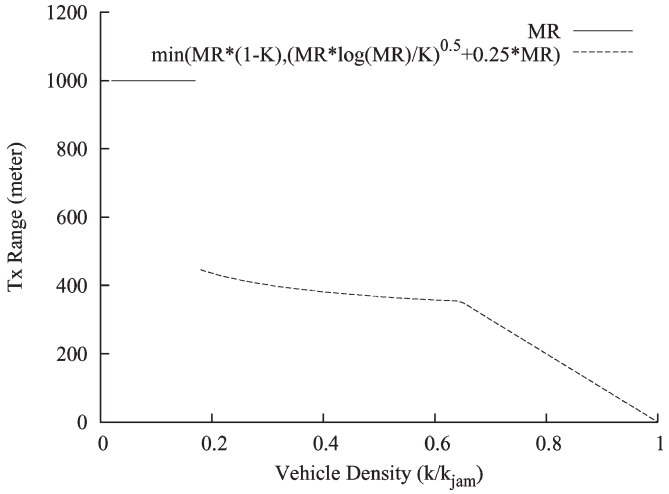

Fig. 7. Values of transmission range returned by the DTRA algorithm versus the estimated vehicle density.

The parameter $\lambda' = \lambda / u_{\max} \approx 0.1$ is determined analytically for the NaSch model, as shown in Table I. The maximum range (MR) depends on the available transmitter power and the specifications of the physical layer.

The MR is also used to replace the road length L in (6) and (7) (lines 7 and 8, respectively). Since a vehicle has no information about the actual road length, the choice of $L = \text{MR}$ is the most practical. This choice will result in some partitioning of the VANET in roads of longer length $(L \gg \text{MR})$. However, the risk of partitioning the network is unavoidable for a finite MR value, as discussed in Section IV. On shorter roads $(L \ll \text{MR})$, the algorithm will overestimate the TR values in congested traffic $(k > k_{\text{c}})$. Section VI-D suggests other practical methods to determine the MR.

Fig. 7 shows the transmission-range values returned by the DTRA algorithm in the entire range of vehicle density, $\text{MR} = L = 1000$ m, and $\alpha = 0.25$.

The choice of the maximum transmission range in free flow is due to two reasons: 1) Estimation of density within the free-flow traffic range is difficult, but it is easy to detect the free-flow phase; 2) it is expected that the distance between vehicles in free flow is long; therefore, a longer than optimal transmission range does not have the same adverse affects as in a dense network, and it can extend the lifetime of communication links as the network topology changes.

Note that a practical algorithm would determine a power level instead of a transmission range. The power level may take any value in a set of possible power levels available to the wireless interface. Here, the algorithm sets the transmission range directly for an easy comparison with the network's length and the distance between vehicles.

C. Performance Evaluation of DTRA Algorithm

The DTRA algorithm described in Algorithm 1 is evaluated using simulations of the four highway configurations described in Section III-B. During the simulations, each vehicle estimates the local density and applies the algorithm to determine its own transmission range. The following metrics are used in the evaluation:

1) Number of network partitions: This is used to measure the network connectivity; a connected network consists of one partition.
2) Average transmission range: The smaller value of the transmission range implies a lesser power level and better network spatial reuse.

To count the number of partitions in the network, 1) an MST is constructed within the measurement section(s) (see below) of the highway in the same way that was used to determine the MTR in Section IV-B. The edges of the MST represent the minimum distance between any two vehicles in the network. 2) Each edge in the MST is checked to determine if it satisfies (4). Otherwise, the network is partitioned at that point, and the number of partitions is increased by one. Note that the procedure results in a network in which all communication links are bidirectional.

In the racetrack configurations (A) and (B) of Section III-B, data collection is restricted to a segment of length $L \approx 1$ km located at the furthest distance from of the entry point so that measurements are not effected by vehicle interactions at that point. In the intersection configurations (C) and (D), data are collected in two 1-km segments immediately upstream and downstream from the intersection.

Fig. 8 shows the average number of partitions and the average transmission range along the density range in different highway configurations. Line and symbol types correspond to different choices for the parameter α in (7), which sets the transmission range in the dense traffic. Fig. 8(a) and (b) shows that the average number of partitions remains very close to one in highway scenarios (A) and (B). The transmission range drops quickly near the critical density while maintaining (or improving) the level of connectivity in racetrack configurations.

Fig. 8(a) and (b) shows the effect of raising the transmission range by a factor of αL. While there is little difference between the choice of $0.25L$ and $0.15L$, the number of partitions increases noticeably at $0L$. The latter sets the range below the mean MTR of the single-lane highway and at roughly the mean MTR in the multilane highway [see Fig. 4(a) and (b) in Section IV-B]. This indicates that the vehicles are able to set their transmission range very close to the optimal value in dense traffic.

The intersection scenarios are challenging for the DTRA algorithm since the network's condition changes rapidly at both sides of the intersection, which requires fast switching of the transmission range from low (while vehicles are slowing or stopped) to high (after passing the intersection). This condition is depicted in Fig. 8(c) and (d) by the absence of data points in the density range [0.1, 0.3] due to the instantaneous change in the vehicle density across the intersection.

Fig. 8(c) and (d) show higher number of partitions across the density range, which can be attributed to the slower reaction to the change in the traffic condition. The figure, which corresponds to a signalized intersection and stop-sign intersections [Configuration (C) and (D), respectively] shows similar results in the high density region. In both cases, the mean headway

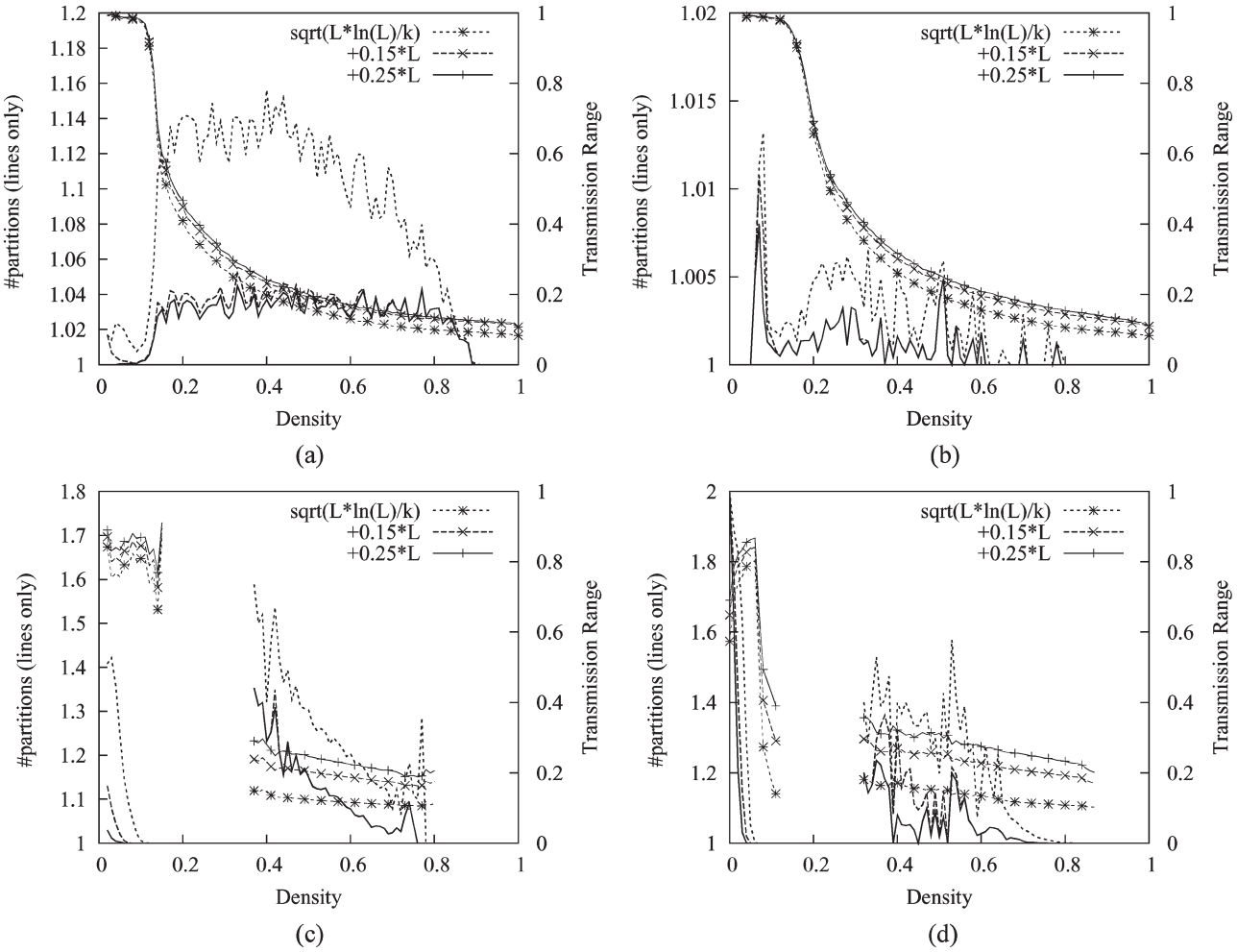

Fig. 8. Vehicle density versus the average transmission range and the resultant number of partitions in (a) one-lane racetrack, (b) three-lane racetrack, (c) signalized intersection, and (d) unsignalized intersection. The lines represent the average number of partitions; the lines/symbols represent the average transmission range (symbols are plotted every fourth point).

(inter arrival time) between vehicles is smaller than the delay encountered at the intersection, which results in a traffic jam upstream from the intersection. The average transmission range in the high-density region [0.4, 0.8] is slightly higher than the corresponding region in the racetrack scenarios, particularly at the lower end. The reason for this difference is the influence of incoming vehicles that approach the intersection with a maximum transmission range (due to free-flow traffic upstream of the intersection) and then decelerate rapidly to join the queue behind the intersection.

Despite the relatively slower reaction to the change in traffic condition, which is expected due to the use of the time window T_t, the DTRA algorithm is quite successful in maintaining the connectivity by keeping the average number of partitions low. Table II offers a detailed description of the network connectivity in each of the above configurations by listing the fraction of time in which the network is connected (one partition) or divided into two, three, or four partitions.

Table II indicates that 1) in the racetrack scenario the upper bound of transmission range given by (7) $(\alpha = 0)$ is sufficient to maintain the network connectivity 95.93% of the time or higher. 2) In the signalized intersection, the increase in the upper bound of transmission range has a significant impact on the connectivity since it increases the time the network is connected by more than 11% upstream of the intersection (the congested side) and about 4% downstream (the free-flow side). It is also noted that the signalized intersection is the only highway configuration where the number of partitions may increase to four. This occurs in the congested area upstream from the intersection. This area is the most dynamic where some vehicles are discharging from the queue in the green-phase while others are joining the queue of stopped vehicles. 3) In the stop-sign intersection [configuration (D)], the congested area upstream from the intersection remains connected most of the time. In the free-flow region downstream, the partitioning of the network is not due to the level of transmission range but is due the slow reaction to the change in traffic conditions.

D. Practical Considerations

It was assumed in Section VI-B that the DTRA algorithm produces its result in the form of a real number that represents a distance. This was intentional in order to compare the results

TABLE II
PERCENTAGE OF PARTITIONS DURING SIMULATION TIME

Road Configuration	α	partitions downstream				partitions upstream			
		1	2	3	4	1	2	3	4
(A) Racetrack (1 lane)	0.00	95.93	3.98	0.08	0.00	N/A			
	0.15	98.75	1.25	0.00	0.00				
	0.25	98.87	1.13	0.00	0.00				
(B) Racetrack (3 lanes)	0.00	99.74	0.25	0.00	0.00	N/A			
	0.15	99.89	0.11	0.00	0.00				
	0.25	99.90	0.10	0.00	0.00				
(C) Signalized Intersection	0.00	95.69	4.30	0.01	0.00	79.91	18.56	1.49	0.05
	0.15	99.77	0.23	0.00	0.00	90.94	8.80	0.26	0.01
	0.25	99.97	0.03	0.00	0.00	90.94	8.79	0.26	0.01
(D) Stop sign Intersection (q_n=600 veh/hr)	0.00	39.01	55.89	5.10	0.00	98.24	1.75	0.01	0.00
	0.15	68.86	31.14	0.00	0.00	99.76	0.24	0.00	0.00
	0.25	82.19	17.81	0.00	0.00	99.77	0.23	0.00	0.00

with the MTR under the same conditions. A practical algorithm will likely produce a power level index that corresponds to one of the power levels settings available for the transmitter. This scheme allows the algorithm to be more flexible for several practical considerations. For instance, in the early stages of VANETs implementation and marketing, only a small percentage of vehicles will be equipped with wireless transceivers. This will make the perceived vehicle density on the highway much less than the actual density because only the equipped vehicles will participate in the VANET. As a result, a certain power index may correspond to a higher power setting when the fraction of equipped vehicles was, for example, 10% than what it would be if the fraction of equipped vehicles was 90%. Since the algorithm is based on the actual vehicle density, which is not affected by the marketing of VANET, the algorithm remains valid and need not to be changed as more vehicles become equipped. The same reasoning also applies to geographic, demographic, or regulatory situations that require the power levels in one region to be different from others.

Moreover, the association between the power index and the actual power level can be determined statically or dynamically.

- The range may be determined statically by, for example, standards. These standards may choose different power levels for different geographic or regulatory regions.
- The range can be estimated directly from traffic models. In this case, the indexes must be set so that at least one corresponds to the free-flow traffic region, while the rest divides the remaining range equally. Algorithm 1 is a special case of this scheme.
- An additional protocol may be used to determine the power range for each index. The protocol does not need to be used as frequently as some of the proposed protocols in the literature since the power level does not change frequently.
- The power level for each index may be determined dynamically by a central authority that broadcasts control messages to vehicles entering a specific region (e.g., highway or city center). This suggests developing a protocol that optimizes power consumption for other factors, such as Quality of Service (QoS), at the region level and then transmits the power level for each index to the vehicles within the region.

VII. CONCLUSION

The main contribution of this paper is the formulation of a local density estimate based on traffic-flow models. This estimate represents a novel approach to predicting vehicle density that depends only on the vehicles' mobility pattern.

One application of the density estimate is the DTRA algorithm. The algorithm sets a vehicle's transmission range dynamically according to its local density. The result of using this algorithm is a VANET whose nodes have a transmission range that is dynamic and nonhomogeneous. Simulations show that the DTRA algorithm is effective in maintaining a high degree of connectivity in highway configurations where the network topology changes rapidly.

The proposed scheme has several advantages. The algorithm does not require any global information such as vehicle locations, nor does it require any exchange of information among vehicles. Moreover, the algorithm inherently adapts to vehicle mobility. The algorithm is also transparent to communication protocols, which allows it to be used in combination with other TPC protocols to enhance their performance with respect to responsiveness to mobility or to provide an initial estimate of transmission range before further refinement.

The ability to estimate the local vehicle density can be useful for many other applications in VANET. Many protocols in *ad hoc* networks are affected by the density of nodes (number of neighbors). For instance, protocols that depend on message broadcast can degrade the network performance due to excessive flooding. Information about local density allows these protocols to adapt their operation to mitigate the negative effects of flooding. Examples may include adjusting the interval between "Hello" beacons according to the change in density, adjusting the routing update interval for proactive routing protocols, or determining the probability of a packet retransmission during message flooding. The local density information does not require any additional overhead and adapts to vehicles' mobility.

Currently, obtaining real-life traces to verify the proposed methods is not feasible for the type and scale of the scenarios presented in this paper. Real-field data must include the position of vehicles in order to obtain transmission-range measurements. This requirement suggests the need for instantaneous observations using video cameras or aerial photography. Therefore, testing the density estimate and the DTRA algorithm using real-field measurements remains an objective for future work.

REFERENCES

[1] J. Gomez and A. T. Campbell, "A case for variable-range transmission power control in wireless multihop networks," in *Proc. 23rd Annu. Joint Conf. INFOCOM*, 2004, vol. 2, pp. 1425–1436.

[2] R. Ramanathan and R. Rosales-Hain, "Topology control of multihop wireless networks using transmit power adjustment," in *Proc. 19th Annu. Joint Conf. INFOCOM*, 2000, vol. 2, pp. 404–413.

[3] L. A. Pipes, "An operational analysis of traffic dynamics," *J. Appl. Phys.*, vol. 24, no. 3, pp. 274–281, Mar. 1953.

[4] S. Ardekani and R. Herman, "Urban network-wide traffic variables and their relations," *Transp. Sci.*, vol. 21, no. 1, pp. 1–16, Feb. 1987.

[5] R. Herman and I. Prigogine, "A two-fluid approach to town traffic," *Science*, vol. 204, no. 4389, pp. 148–151, Apr. 13, 1979.

[6] K. Nagel and M. Schreckenberg, "A cellular automaton model for freeway traffic," *J. Phys., I France*, vol. 2, no. 12, pp. 2221–2229, Dec. 1992.

[7] M. M. Artimy, W. Robertson, and W. J. Phillips, "Vehicle traffic microsimulator for *ad hoc* networks research," in *Proc. IWWAN*, Oulu, Finland, May 2004, pp. 105–109.

[8] F. L. Hall. (1997). "Traffic stream characteristics," in *Traffic Flow Theory: A State of the Art Report—Revised Monograph on Traffic Flow Theory*, N. H. Gartner, C. Messer, and A. K. Rathi, Eds. Oak Ridge, TN: Oak Ridge Nat. Lab., ch. 2. [Online]. Available: http://www.tfhrc.gov/its/tft/tft.htm

[9] R. Haberman, *Mathematical Models: Mechanical Vibrations, Population Dynamics, and Traffic Flow: An Introduction to Applied Mathematics*. Englewood Cliffs, NJ: Prentice-Hall, 1977.

[10] R. W. Rothery. (1997). "Car-following models," in *Traffic Flow Theory: A State of the Art Report—Revised Monograph on Traffic Flow Theory*, N. H. Gartner, C. Messer, and A. K. Rathi, Eds. Oak Ridge, TN: Oak Ridge Nat. Lab., ch. 4. [Online]. Available: http://www.tfhrc.gov/its/tft/tft.htm

[11] R. Kuhne and P. Michalopoulos. (1997). "Continuum flow models," *Traffic Flow Theory: A State of the Art Report—Revised Monograph on Traffic Flow Theory*. Oak Ridge, TN: Oak Ridge Nat. Lab. [Online]. Available: http://www.tfhrc.gov/its/tft/tft.htm

[12] T. Nagatani, "The physics of traffic jams," *Rep. Prog. Phys.*, vol. 65, no. 9, pp. 1331–1386, Sep. 2002.

[13] D. Jost and K. Nagel, "Probabilistic traffic flow breakdown in stochastic car following models," *Transp. Res. Rec.*, no. 1852, pp. 152–158, 2003.

[14] K. Nagel, P. Wagner, and R. Woesler, "Still flowing: Approaches to traffic flow and traffic jam modeling," *Oper. Res.*, vol. 51, no. 5, pp. 681–710, Sep./Oct. 2003.

[15] P. Santi and D. M. Blough, "An evaluation of connectivity in mobile wireless *ad hoc* networks," in *Proc. Int. Conf. Dependable Syst. Netw.*, Jun. 2002, pp. 89–98.

[16] M. Desai and D. Manjunath, "On the connectivity in finite *ad hoc* networks," *IEEE Commun. Lett.*, vol. 6, no. 10, pp. 437–439, Oct. 2002.

[17] Y. C. Cheng and T. G. Robertazzi, "Critical connectivity phenomena in multihop radio models," *IEEE Trans. Commun.*, vol. 37, no. 7, pp. 770–777, Jul. 1989.

[18] O. Dousse, P. Thiran, and M. Hasler, "Connectivity in *ad-hoc* and hybrid networks," in *Proc. 21st Annu. Joint Conf. INFOCOM*, 2002, vol. 2, pp. 1079–1088.

[19] M. M. Artimy, W. Robertson, and W. J. Phillips, "Minimum transmission range in vehicular *ad hoc* networks over uninterrupted highways," in *Proc. IEEE ITSC*, 2006, pp. 1400–1405.

[20] J. J. Blum, A. Eskandarian, and L. J. Hoffman, "Challenges of intervehicle *ad hoc* networks," *IEEE Trans. Intell. Transp. Syst.*, vol. 5, no. 4, pp. 347–351, Dec. 2004.

[21] Z. D. Chen, H. T. Kung, and D. Vlah, "*Ad hoc* relay wireless networks over moving vehicles on highways," in *Proc. 2nd ACM Int. Symp. Mobile Ad Hoc*, Long Beach, CA, 2001, pp. 247–250.

[22] T. Kosch, C. Schwingenschlogl, and L. Ai, "Information dissemination in multihop inter-vehicle networks," in *Proc. IEEE 5th ITSC*, 2002, pp. 685–690.

[23] M. Rudack, M. Meincke, K. Jobmann, and M. Lott, "On traffic dynamical aspects of inter vehicle communications (IVC)," in *Proc. 58th IEEE Semiannu. VTC—Fall*, 2003, vol. 5, pp. 3368–3372.

[24] H. Füßler, M. Mauve, H. Hartenstein, D. Vollmer, and M. Käsemann, "A comparison of routing strategies in vehicular *ad-hoc* networks," *Reihe Informatik*, Mar. 2002.

[25] M. Rudack, M. Meincke, and M. Lott, "On the dynamics of *ad hoc* networks for inter vehicles communications (IVC)," in *Proc. Int. Conf. Wireless Netw.*, Las Vegas, NV, Jun. 2002, pp. 33–39.

[26] M. D. Penrose, "The longest edge of the random minimal spanning tree," *Ann. Appl. Probab.*, vol. 7, no. 2, pp. 340–361, May 1997.

[27] L. Wischhof, A. Ebner, and H. Rohling, "Information dissemination in self-organizing intervehicle networks," *IEEE Trans. Intell. Transp. Syst.*, vol. 6, no. 1, pp. 90–101, Mar. 2005.

[28] M. M. Artimy, "Modelling of transmission range in vehicular *ad hoc* networks," Ph.D. dissertation, Dalhousie Univ., Halifax, NS, Canada, 2006.

[29] P. Santi, "Topology control in wireless *ad hoc* and sensor networks," *ACM Comput. Surv.*, vol. 37, no. 2, pp. 164–194, Jun. 2005.

[30] N. Li, J. C. Hou, and L. Sha, "Design and analysis of an MST-based topology control algorithm," in *Proc. 22nd Annu. Joint Conf. INFOCOM*, 2003, vol. 3, pp. 1702–1712.

[31] R. Wattenhofer, L. Li, P. Bahl, and Y. M. Wang, "Distributed topology control for power efficient operation in multihop wireless *ad hoc* networks," in *Proc. 20th Annu. Joint Conf. INFOCOM*, 2001, vol. 3, pp. 1388–1397.

[32] L. Li, J. Y. Halpern, P. Bahl, Y.-M. Wang, and R. Wattenhofer, "A cone-based distributed topology-control algorithm for wireless multi-hop networks," *IEEE/ACM Trans. Netw.*, vol. 13, no. 1, pp. 147–159, Feb. 2005.

[33] J. Liu and B. Li, "MobileGrid: Capacity-aware topology control in mobile *ad hoc* networks," in *Proc. 11th Int. Conf. Comput. Commun. Netw.*, 2002, pp. 570–574.

[34] M. Krunz, A. Muqattash, and S.-J. Lee, "Transmission power control in wireless *ad hoc* networks: Challenges, solutions and open issues," *IEEE Netw.*, vol. 18, no. 5, pp. 8–14, Sep./Oct. 2004.

[35] E. C. Arvelo, "Open-loop power control based on estimations of packet error rate in a Bluetooth radio," in *Proc. IEEE WCNC*, 2003, vol. 3, pp. 1465–1469.

Maen Artimy (S'98–M'06) received the B.Sc. degree in computer engineering from Al-Fateh University, Tripoli, Libya, in 1990 and the M.A.Sc. degree in electrical engineering, as well as the Ph.D. degree, from Dalhousie University, Halifax, NS, Canada, in 1999 and 2006, respectively.

Prior to his postgraduate study, he held positions in the IT industry and is currently the Senior Network Designer at Internetworking Atlantic Inc. and a Lecturer at the Internetworking Program at Dalhousie University, both in Halifax. His research interests include Vehicular *Ad Hoc* Networks and Inter networking technologies.

Dr. Artimy is a member of the Association of Professional Engineers of Nova Scotia.